science, engineering and health studies

Research Article

Science, Engineering and Health Studies
https://lio1.tci-thaijo.org/index.php/sehs
ISSN (Online): 2630-0087

Synergistic activity of friedelan-3β-ol isolated from *Euphorbia lactea* and doxorubicin against MDA-MB-231 breast cancer cell line

Supusson Pengnam[1,2], Pawaris Wongprayoon[1,3], Panupun Limpachayaporn[4], Kanok-on Rayanil[4] and Purin Charoensuksai[1,3]*

[1] Department of Biomedicine and Health Informatics, Faculty of Pharmacy, Silpakorn University, Nakhon Pathom 73000, Thailand
[2] Green Innovations Group (PDGIG), Faculty of Pharmacy, Silpakorn University, Nakhon Pathom 73000, Thailand
[3] Bioactives from Natural Resources Research Collaboration for Excellence in Pharmaceutical Sciences, Faculty of Pharmacy, Silpakorn University, Nakhon Pathom 73000, Thailand
[4] Department of Chemistry, Faculty of Science, Silpakorn University, Nakhon Pathom 73000, Thailand

ABSTRACT

The cytotoxic activity of three triterpenoid compounds namely, friedelin **[1]**, friedelan-3β-ol **[2]** and taraxerol **[3]** isolated from hexane fraction *Euphorbia lactea* Haw. was investigated in breast cancer cell lines MDA-MB-231 and MCF-7. Dose-dependent cytotoxic activity of these compounds was detected in MDA-MB-231 cells. Of the three compounds, **[2]** elicited the strongest inhibitory effect. The interplay between **[2]** and doxorubicin (Dox) in a series of combination treatments was analyzed in MDA-MB-231. Computer modeling software CompuSyn revealed that **[2]** and Dox exhibited a synergistic relationship over a broad range of concentration. The ratio of **[2]**:Dox at 25:1 µg/mL was predicted to achieve a 90% inhibitory effect with the lowest dose of each agent, thus allowing a dose reduction of **[2]** and Dox by ~30 and ~3 fold, respectively. Finally, the percentage of apoptotic cells in MDA-MB-231 treated with **[2]**:Dox at a 25:1 µg/mL combination was markedly higher than cells treated with 1x and 2x the concentration of each individual agent, supporting the predicted synergism. Together, the results highlighted **[2]** as an anticancer phytochemical exhibiting synergistic activity with Dox and warranted further research to assess the possibility to exploit this synergy for breast cancer treatment.

***Corresponding author**:*
Purin Charoensuksai
charoensuksai_p@su.ac.th

***Received**: 27 May 2022*
***Revised**: 1 June 2022*
***Accepted**: 8 August 2022*
***Published**: 18 October 2022*

***Citation**:*
Pengnam, S., Wongprayoon, P., Limpachayaporn, P., Rayanil, K., and Charoensuksai, P. (2022). Synergistic activity of friedelan-3β-ol isolated from Euphorbia lactea and doxorubicin against MDA-MB-231 breast cancer cell line. Science, Engineering and Health Studies, 16, 22050011.

Keywords: *Euphorbia lactea*; friedelan-3β-ol; combination; anticancer; triterpenoid; CompuSyn

1. INTRODUCTION

Globally, breast cancer accounts for approximately 30% of all cancer cases in women and is ranked the second most common cancer-related death in women (Siegel et al., 2020). The pathology of breast cancer involves various risk factors such as advancing age, genetic mutation and familial history (Loibl et al., 2021). Current breast cancer therapy includes radiotherapy, surgery and pharmacotherapy (Maughan et al., 2010). However, drug resistance and adverse drug reactions can detrimentally affect treatment. Therefore, the discovery and development

of new anticancer agents against breast cancer are much needed.

Euphorbia, belonging to the botanical family Euphorbiaceae, consists of over 2000 species of flowering plants. A number of publications have revealed that euphorbia contains a wide repertoire of phytochemicals with diverse pharmacological activities including antimicrobial, anti-inflammatory and anticancer properties (Ernst et al., 2015; Shi et al., 2008). Along with at least 500 compounds isolated from this group of plants, euphorbia appears to be a rich source of terpenoids (Shi et al., 2008). Moreover, many of these terpenoids have been shown to exert an inhibitory effect against diverse models of cancer (Wongrakpanich and Charoensuksai, 2018).

A standard pharmacological treatment for breast cancer involves a combination of multiple drugs, which can confer benefits including a higher probability to achieve favorable response, decrease dosages, lessen the associated risk of concentration-dependent adverse effects, and prevent drug resistance (Fisusi and Akala, 2019). Doxorubicin (Dox), an anthracycline drug, is one of the most frequently used chemotherapeutic agents for breast cancer. In practice, Dox is often used in combination with other chemotherapeutic agents including cyclophosphamide, 5-fluorouracil, paclitaxel, docetaxel and mitomycin (Fisusi and Akala, 2019; Gradishar et al., 2020; Maughan et al., 2010).

Our research team has previously detected anti-proliferative and anti-migratory effects of *Euphorbia lactea* Haw. hydroalcoholic extract against HN22 cell line (Wongprayoon and Charoensuksai, 2018). This prompted us to continue the investigation to understand whether putative cytotoxic compound(s) can be isolated from this plant and if it can confer advantages when used in combination with established anticancer compounds. However, the interpretation of the interaction of drugs in a combination treatment, i.e., synergistic, additive and antagonistic effect, is largely affected by the definition of each term from the perspective of the observer. To avoid this bias, we utilized CompuSyn software which employed the Chou-Talalay algorithm to calculate, predict and determine the interplay between drugs when used simultaneously in a combination strategy.

2. MATERIALS AND METHODS

2.1 Materials

Dox hydrochloride and 3-(4,5-dimethylthiazol-2-yl)-2,5-diphenyl tetrazolium bromide (MTT) were bought from Sigma Aldrich® (St. Louis, MO, USA). Hoechst 33342 trihydrochloride and SYTOX® green were purchased from Invitrogen (Carlsbad, California, USA). Breast cancer cell lines, MCF-7 and MDA-MB-231 were obtained from American Type Culture Collection (ATCC, Rockville, MD, USA). Dulbecco's modified Eagle medium (DMEM), trypsin-EDTA, penicillin/streptomycin antibiotics (Pen/Strep), and fetal bovine serum (FBS) were purchased from GIBCO (San Diego, California, USA). Dimethyl sulfoxide (DMSO) was purchased from Fisher Scientific (Waltham, MA, USA). Hydroxypropyl-β-cyclodextrin (Cavasol W7 HP Pharma) was purchased from Wacker Chemie AG (Munich, Germany). Information regarding the structural identification of compounds **[1-3]** can be found in supplementary materials.

2.2 Determination of anticancer activity by MTT assay

MCF-7 and MDA-MB-231 were cultured in DMEM supplemented with 10% FBS and 1% Pen/Strep at 37°C and 5% CO_2. The isolated compounds **[1-3]** were dissolved in a solution mixture containing DMSO and 30% w/v hydroxypropyl-β-cyclodextrin (DMSO-HPBCD). The anticancer activity of isolated compounds was tested in MCF-7 and MDA-MB-231. Cells were exposed to isolated compounds at 2.5, 5, 10, 25 and 50 µg/mL final concentration. For the combination experiment, MDA-MB-231 cells were treated with **[2]** and Dox at various concentrations and ratios. First, cells were treated with a fixed concentration of Dox at 0.1 µg/mL while the concentration of **[2]** varied from 2.5-50 µg/mL. Next, cells were treated with a fixed concentration of **[2]** at 25 µg/mL while the concentration of Dox varied from 0.01-1 µg/mL. The final concentration of DMSO-HPBCD vehicle control was maintained at 0.5% w/v for all conditions. Cells were exposed to the compounds for 72 h. Afterward, cell viability was determined by MTT assay.

For MTT assay, once the cells reached the designated exposure time, the stock solution of MTT was added into each well to the final concentration of 1 mg/mL and incubated for 3 h. Then, the medium was discarded and 100 μL DMSO was added to each well before measuring the amount of formazan by UV-Vis VICTOR Nivo multimode microplate reader (PerkinElmer Inc., Waltham, MA, USA) at 550 nm. Data were presented as the percentage of cell viability relative to vehicle control. All experiments were performed in triplicate.

2.3 Combination index (CI) and dose reduction index (DRI) analysis

Cell viability data of the combination experiments was used to calculate fractional inhibition (Fa = 100 – % cell viability of sample)/100) and then analyzed by CompuSyn software (Bijnsdorp et al., 2011; Chou, 2010). The anticancer interaction between **[2]** and Dox was determined by the CI method to identify synergistic (CI<1), additive (CI=1), and antagonistic relationships (CI>1). DRI was calculated as a fold reduction in individual drug dose in single treatments relative to its dose in combination in order to reach the same inhibitory effect. DRI > 1 favored dose reduction whereas DRI < 1 disfavored dose reduction.

2.4 Analysis of cells undergoing apoptosis

MDA-MB-231 cells were plated in a 96-well plate at 6,000 cells/well and allowed to attach. Cells were then exposed to 25 µg/mL of **[2]** and 1 µg/mL of Dox in a combination treatment (ratio of **[2]**:Dox = 25:1). Additionally, cells were exposed to 1x and 2x the concentrations of **[2]** and Dox in a single treatment. Cells were exposed to the tested compounds for 24 h. Afterward, Hoechst 33342 (5 mg/mL in PBS) and SYTOX® green (0.1 µM in PBS) were used to stain DNA and dead cells, respectively. Cells were stained for 15 min while protected from light. Nucleus morphology of MDA-MB-231 cells was observed by an inverted fluorescent microscope (Eclipse TE 2000-U, Nikon, Yokohama, Japan) with DAPI and blue excitation (B-2A) filter for Hoechst 33342 and SYTOX® green, respectively. A bar graph represents apoptotic cells with characteristic nuclear condensation and fragmentation when stained with Hoechst 33342 normalized to the total number of

cells within the same microscopic field. Data were collected from three different microscopic fields. Error bars represent standard deviation.

2.5 Data analysis

All data were expressed as means and standard deviations. Statistical analysis used for each stage of the study was described in each figure. GraphPad Prism software version 7 was used for statistical analysis and p-value < 0.05 was considered statistically significant.

3. RESULTS AND DISCUSSION

Previously, our group reported that crude ethanolic extract of *E. lactea* exhibited cytotoxic activity against HN22 cancer cells (Wongprayoon and Charoensuksai, 2018). This observation led to the investigation of whether the cytotoxic activity could be extended to other cancer cell types and whether putative cytotoxic compound(s) could be isolated from this plant. Then polarity-based fractionation and purification was employed which resulted in the isolation of three triterpenoid compounds; namely, friedelin **[1]**, friedelan-3β-ol **[2]** and taraxerol **[3]** from the hexane fraction of *E. lactea* (Figure 1). Chemical structure elucidation of these compounds was performed by 1D and 2D-NMR spectroscopic data and by comparing their physical and spectroscopic data with other reported literature (Govindachari et al., 1967; Jamal et al., 2009; Koay et al., 2013; Ndwigah et al., 2013). Moreover, the molecular mass of the isolated compounds measured by HRESIMS was consistent with the calculated mass of each compound.

The cytotoxic activity of these compounds was first determined in two breast cancer cell lines, i.e., MDA-MB-231 and MCF-7 cell lines. At 72 h of exposure, all compounds exhibited a dose-dependent cytotoxic activity against MDA-MB-231 cells, while the marginal effect was observed in MCF-7 (Figure 2). Of the three compounds, **[2]** exhibited the most potent cytotoxic activity, achieving ~40% reduction in cell viability at 50 µg/mL. It should also be noted that the molecular mass of the three compounds was nearly identical (~450 g/mole).

Given that pharmacological treatment of cancer often employs multiple anticancer agents in a co-treatment strategy, we then asked whether **[2]** could potentiate the effect of other anticancer compounds routinely used for the management of breast cancer. Dox was selected as a model drug. To investigate the effect of **[2]** in combination with Dox, a series of co-treatments was carried out in MDA-MB-231 fixing the concentration of one agent while varying the concentration of the other and vice versa. First, the concentration of Dox was fixed at 0.1 µg/mL while the concentration of **[2]** was varied from 2.5-50 µg/mL (Figure 3A). Afterward, the concentration of **[2]** was fixed at 25 µg/mL, while the concentration of Dox was varied from 0.01-1 µg/mL (Figure 3B). The results revealed that the addition of **[2]** increased the cytotoxic activity of the treatment in all tested conditions. Notably, the potentiation effect appeared to be stronger on increasing Dox concentration, achieving >80% reduction in cell viability at conditions 25:0.5 and 25:1 **[2]**:Dox ratio (Figure 3B), while such effects appeared to diminish on increasing the concentration of **[2]** (Figure 3A). Morphological changes, i.e., decreased density, cell shrinkage and detachment of MDA-MB-231 that were treated with **[2]** and Dox combinations at 25:0.5 and 25:1 **[2]**:Dox ratio (Figure 3C)were consistent with the marked decrease in cell viability of the combination treatment compared to the single agent as determined by MTT assay.

To further understand the interplay between **[2]** and Dox, data collected from the combination treatment were subjected to analysis by computer modeling software CompuSyn (Chou, 2010). First, our team sought to determine whether **[2]** and Dox exhibited synergistic activity. Indeed, the analysis revealed that **[2]** and Dox exhibited a synergistic effect under all test conditions (Table 1). Further, the strongest synergistic effect, as demonstrated by the low CI value, was predicted in 25:0.5 and 25:1 **[2]**:Dox ratio (Table 1).

Next, to determine which combination ratio would likely perform best over a range of concentration, data collected from the 25:1, 50:1, 250:1 and 500:1 **[2]**:Dox combination treatments were analyzed by CompuSyn. The results revealed that 25:1 **[2]**:Dox ratio emerged as the best combination as it was predicted to achieve the highest inhibitory effect (Fa) (Figure 4A), while maintaining the synergy over a broad range of concentration (Figure 4B). Moreover, among the four combination ratios tested, the predicted concentration of each agent required to reach 90% inhibition (0.9 Fa) was the lowest in the 25:1 **[2]**:Dox combination (Table 2). At this ratio, the concentration of **[2]** and Dox required to reach 90% inhibition was predicted to be ~30 and ~3 folds lower than the concentration of **[2]** or Dox when used as a single agent in order to reach the same effect, respectively.

As the cell viability assay and computer modeling prediction favored this condition, the 25:1 **[2]**:Dox ratio was selected for further analysis to determine the percentage of cells undergoing apoptosis using a fluorescent imaging technique. In this analysis, cells undergoing apoptosis, which exhibited nuclear condensation and fragmentation were stained bright blue with Hoechst 33342 (Figure 5A) compared to healthy living cells. Dead cells with compromised integrity of the cell membrane appeared green with SYTOX® green staining. Indeed, apoptotic cells markedly increased in MDA-MB-231 treated with the combination of **[2]** and Dox at 25 µg/mL and 1 µg/mL (25:1), respectively, compared to the vehicle control (Figure 5B). The increase in the proportion of apoptotic cells of the combination was significantly more than each individual agent when used at the same concentration (1x) in the single treatment. Notably, the induction of apoptosis of the combination was higher than **[2]** or Dox at twice the concentration (2x; 50 µg/mL for **[2]** and 2 µg/mL for Dox) when used as a single agent (Figure 5B).

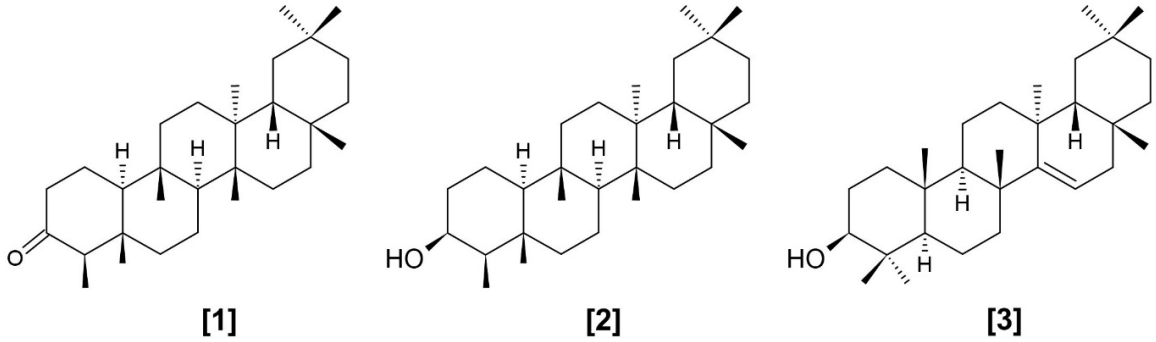

Figure 1. Chemical structures of friedelin **[1]**, friedelan-3β-ol **[2]** and taraxerol **[3]** isolated from the hexane extract of *E. lactea*

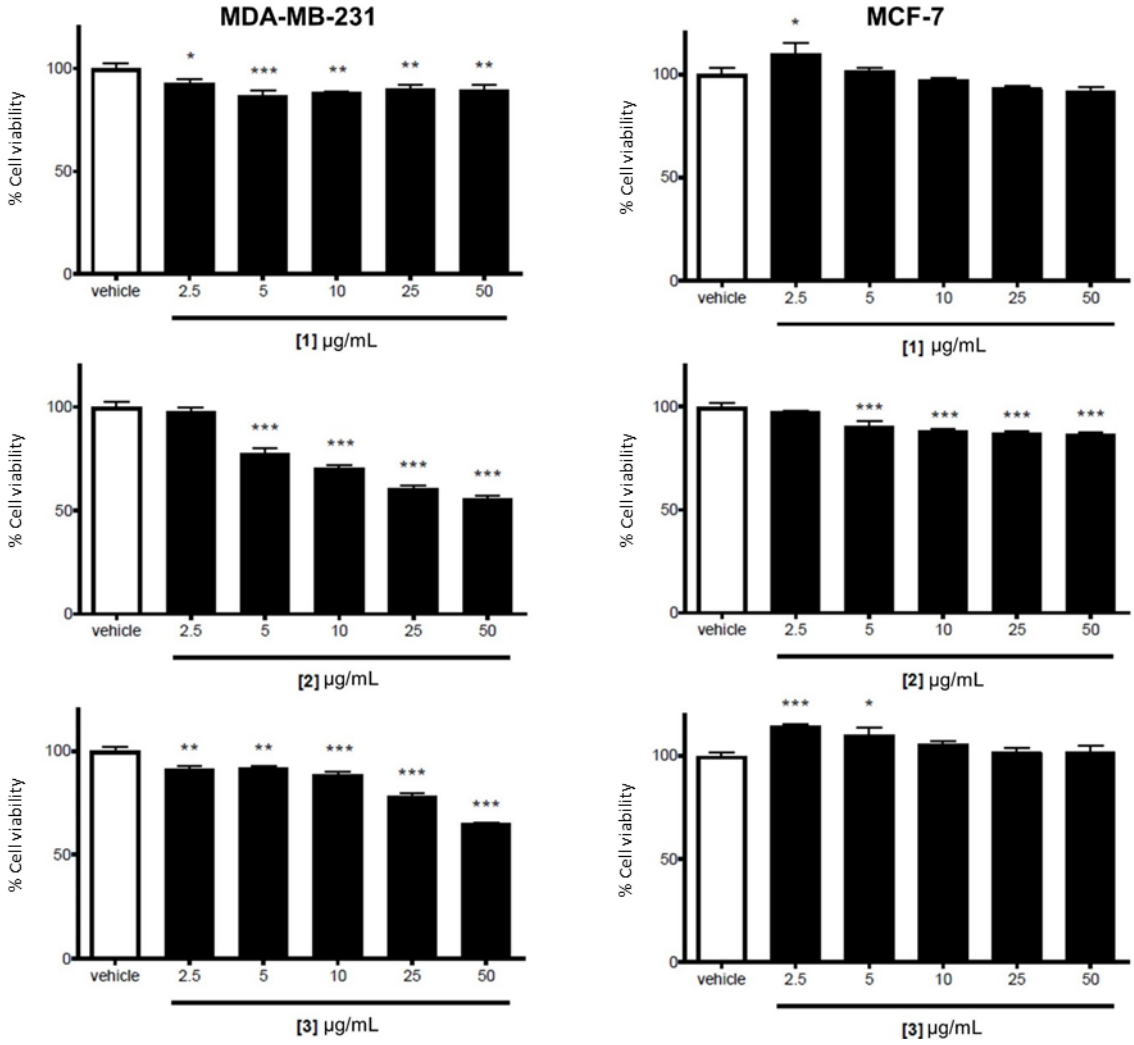

Figure 2. Dose-dependent cytotoxic activity of triterpenoids isolated from *E. lactea* against MDA-MB-231 cells after 72 h exposure

Note: Statistical significance was calculated using one-way ANOVA with Fisher's LSD test.

$^{***}p < 0.001$, $^{**}p < 0.01$, and $^{*}p < 0.05$ compared with vehicle control.

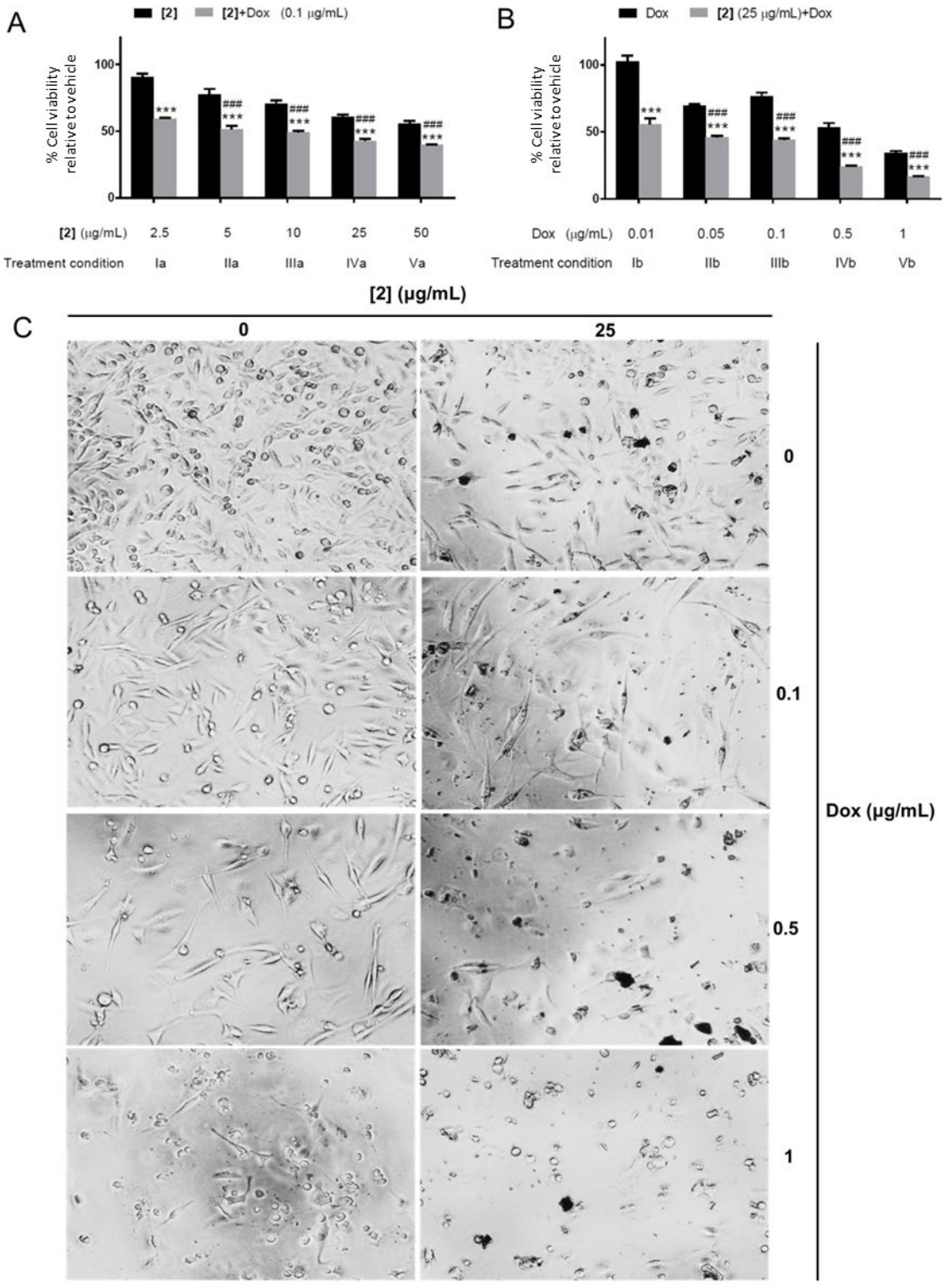

Figure 3. The anticancer activity of **[2]** and Dox combination treatment in MDA-MB-231 cells; (A) viability of cells exposed to a series of combination treatments with a constant concentration of dox (0.1 μg/mL) and a varying concentration of **[2]** (2.5, 5, 10, 25 and 50 μg/mL), (B) viability of cells exposed to a series of combination treatments with a constant concentration of **[2]** (25 μg/mL) and a varying concentration of Dox (0.01, 0.05, 0.1, 0.5 and 1 μg/mL), (C) morphology of MDA-MB-231 cells after 72 h of Dox exposure with and without **[2]** under an inverted microscope

Note: Statistical significance was calculated using two-way ANOVA with Fisher's LSD tests. $^{***}p < 0.001$ compared with the single agent treatment (the adjacent black bar), $^{###}p < 0.001$ compared with the co-treatment condition Ia for Figure A and Ib for Figure B (the furthest left gray bar), respectively.

Table 1. The combination index of **[2]** and Dox at various ratios generated by CompuSyn

Treatment conditions[1]	Ratio of [2]:Dox	Concentration (µg/mL)		Fractional inhibition (Fa)	Combination index (CI)	Grade of CI[2]
		[2]	Dox			
Ia	25:1	2.5	0.1	0.41	0.48	+++
IIa	50:1	5	0.1	0.48	0.37	+++
IIIa	100:1	10	0.1	0.51	0.41	+++
IVa	250:1	25	0.1	0.57	0.46	+++
Va	500:1	50	0.1	0.60	0.64	+++
Ib	2500:1	25	0.01	0.45	0.68	+++
IIb	500:1	25	0.05	0.54	0.46	+++
IIIb	250:1	25	0.10	0.55	0.51	+++
IVb	50:1	25	0.50	0.76	0.36	+++
Vb	25:1	25	1.00	0.83	0.34	+++

Note: [1] corresponding with the treatment conditions depicted in Figure 3.

[2] CI values interpretation as follows: <0.1 very strong synergism (+++++), 0.1–0.3 strong synergism (++++), 0.3–0.7 synergism (+++), 0.7–0.85 moderate synergism (++), 0.85–0.90 slight synergism (+), 0.90–1.10 nearly additive (±), 1.10–1.20 slight antagonism (-), 1.20–1.45 moderate antagonism (--), 1.45–3.3 antagonism (---), 3.3–10 strong antagonism (----), >10 very strong antagonism (-----).

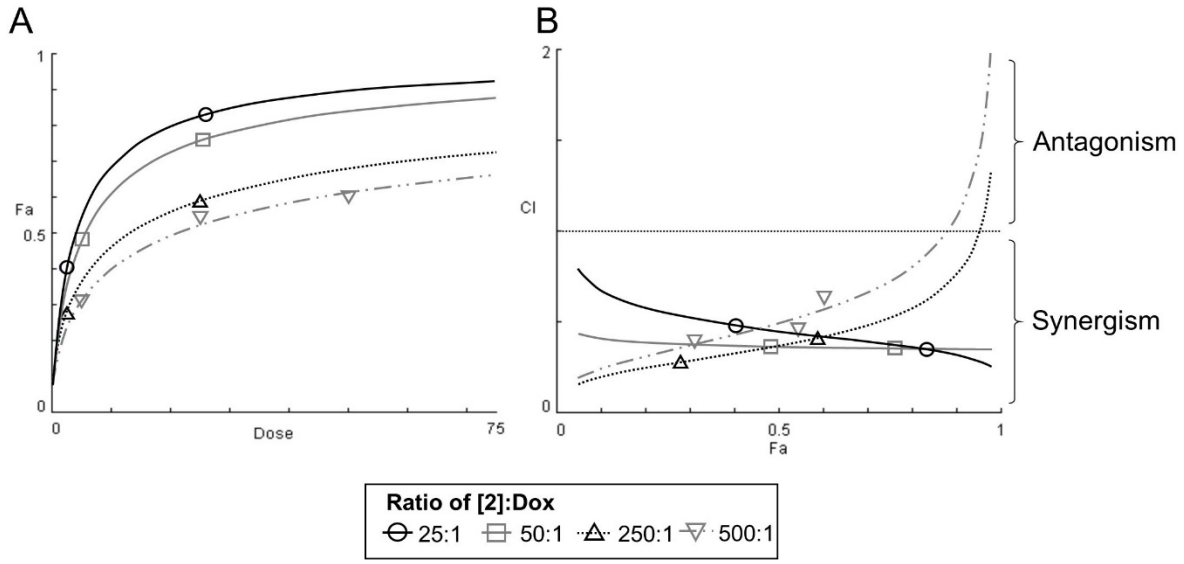

Figure 4. Graphical representations of combination treatment at the ratio 25:1, 50:1, 250:1 and 500:1 generated by CompuSyn software; (A) dose-effect curve and (B) combination index plot

Table 2. Simulation data obtained from CompuSyn software predicting the concentration of each individual agent required to reach 90% cell inhibition (IC_{90}), combination indexes (CIs) and dose reduction indexes (DRIs) of each agent at different combination ratios

Samples	CI	Concentration for IC_{90} (µg/mL)		DRI of [2]	DRI of Dox
		[2]	Dox		
[2]		1668.24			
Dox			6.76		
25:1	0.32	49.05	1.96	34.01	3.44
50:1	0.35	98.85	1.98	16.88	3.42
250:1	0.77	643.90	2.56	2.59	2.62
500:1	1.10	1224.96	2.45	1.36	2.76

Our report served as a proof-of-concept that **[2]** could be used in combination with Dox against breast cancer, conferring a synergistic effect and favoring a dose-reduction of Dox at least in MDA-MB-231 cell line. Nevertheless, breast cancers are generally classified into molecular subtypes including hormone receptor sensitive, HER2 positive and triple negative subclasses (Jeibouei et al., 2019) with specific treatment schemes for each group. Indeed, this data indicated that the inhibitory effect of **[2]** was more prominent against the MDA-MB-231 (triple negative type) than the MCF-7 (hormone receptor sensitive type). It will be interesting to investigate the effect of **[2]**, alone and in combination with other anticancer agents, using established cancer cell lines representing specific subclasses of breast cancer (Dai et al., 2017).

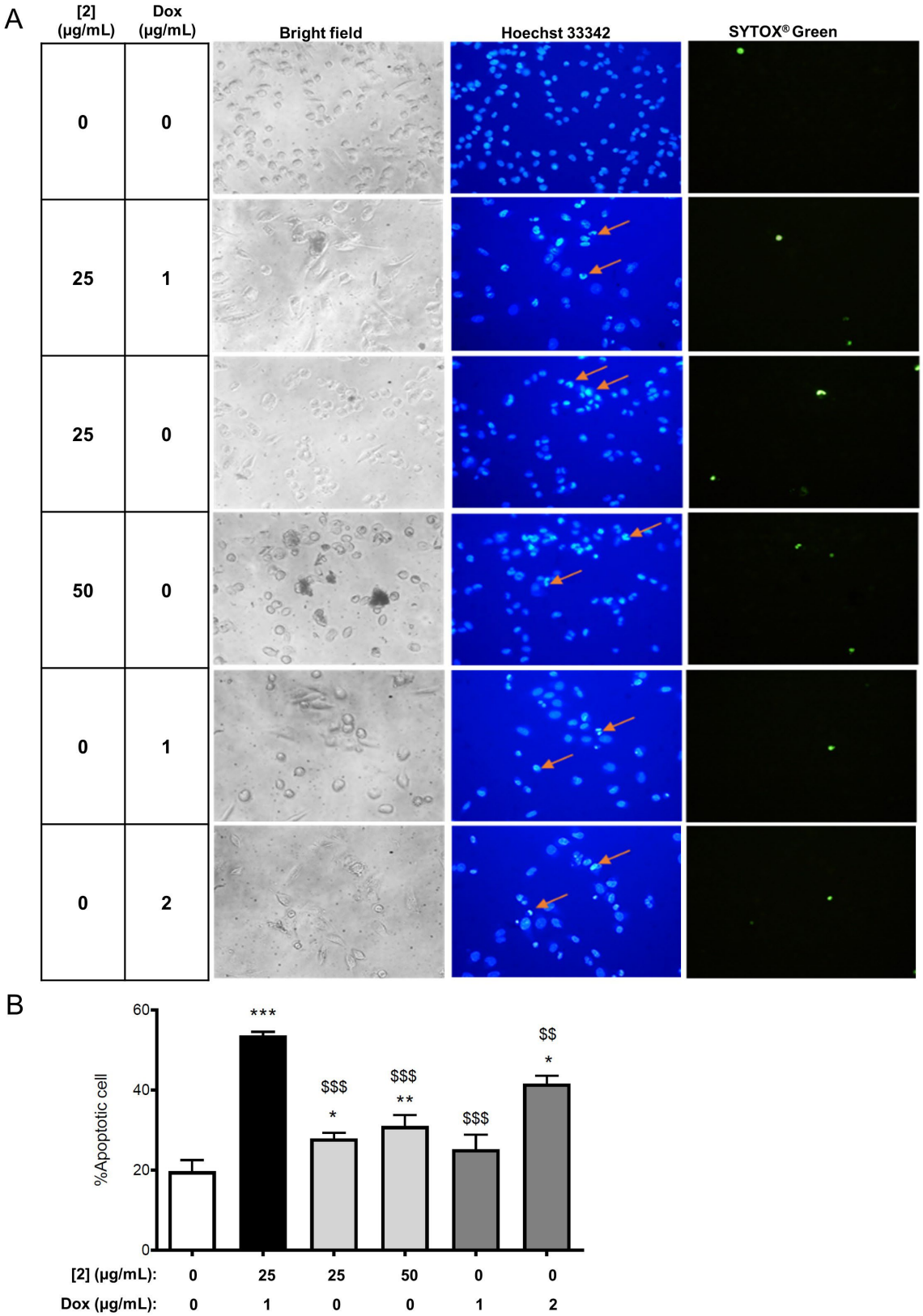

Figure 5. Determination of cells undergoing apoptosis after 24 h of being treated by double staining with Hoechst 33342 and SYTOX® green; (A) representative images from an inverted fluorescent microscope (arrows indicate apoptotic cells), (B) percentage of cells undergoing apoptosis (apoptotic cells were counted and normalized to the total number of cells in the same field)

Note: Statistical significance was calculated using one-way ANOVA with Fisher's LSD test. ***$p < 0.001$, **$p < 0.01$, *$p < 0.05$ compared with the vehicle (White bar); $$$ $p < 0.001$, $$ $p < 0.01$, $ $p < 0.05$ compared with **[2]**:Dox 25:1 μg/mL (Black bar).

Previous reports indicated that **[2]** generally exerted a weak cytotoxic activity against several cancer cell lines (Monkodkaew et al., 2009; Oliveira et al., 2012; Su et al., 2009); however, strong effects were detected in certain cancer types, such as Kaposi sarcoma cell line (~30% inhibition at 20 μM) (Martucciello et al., 2010) and T24 bladder cancer cell line (50% inhibition at 35 ~μM) (Yessoufou et al., 2015). Therefore, it may be worthwhile to explore the cytotoxic activity of this compound in combination with established anticancer agents routinely used to treat these cancers.

4. CONCLUSION

This report described the cytotoxic activity of friedelan-3β-ol or **[2]**, a triterpenoid isolated from *Euphorbia lactea* Haw. against breast cancer. Compound **[2]** exhibited a dose-dependent cytotoxic activity against MDA-MB-231 breast cancer cell line, and a synergistic activity with a chemotherapeutic agent Dox over a broad range of concentrations. Computer modeling predicted that a combination of **[2]**:Dox at 25 μg/mL and 1 μg/mL could achieve a 90% inhibitory effect with the lowest dose of each agent, allowing the dose reduction of **[2]** and Dox by ~30 and ~3 folds, respectively. Finally, the synergistic effect of the combination was further confirmed by the analysis of cells undergoing apoptosis.

ACKNOWLEDGMENT

This publication is a part of research project "The development of natural products for the treatment of age-related diseases" (SURIC 62/01/43) funded by the National Research Council of Thailand through Silpakorn University Research, Innovation and Creativity Administration Office (SURIC). We thank the Faculty of Pharmacy, Silpakorn University for research facilities and instruments. We thank Prof. Praneet Opanasopit for cell lines and reagents. We thank Dr. John Tigue for English language edition and critical reading of the manuscript.

REFERENCES

Bijnsdorp, I. V., Giovannetti, E., and Peters, G. J. (2011). Analysis of drug interactions. In *Cancer Cell Culture* (Cree, I. A., ed.), 2nd, pp. 421-434. Totowa, New Jersey: Humana Press.

Chou, T. C. (2010). Drug combination studies and their synergy quantification using the Chou-Talalay method. *Cancer Research*, 70(2), 440-446.

Dai, X., Cheng, H., Bai, Z., and Li, J. (2017). Breast cancer cell line classification and its relevance with breast tumor subtyping. *Journal of Cancer*, 8(16), 3131-3141.

Ernst, M., Grace, O. M., Saslis-Lagoudakis, C. H., Nilsson, N., Simonsen, H. T., and Rønsted, N. (2015). Global medicinal uses of *Euphorbia L.* (Euphorbiaceae). *Journal of Ethnopharmacology*, 176, 90-101.

Fisusi, F. A., and Akala, E. O. (2019). Drug combinations in breast cancer therapy. *Pharmaceutical Nanotechnology*, 7(1), 3-23.

Govindachari, T. R., Viswanathan, N., Pai, B. R., Rao, U. R., and Srinivasan, M. (1967). Triterpenes of *Calophyllum inophyllum* Linn. *Tetrahedron*, 23(4), 1901-1910.

Gradishar, W. J., Anderson, B. O., Abraham, J., Aft, R., Agnese, D., Allison, K. H., Blair, S. L., Burstein, H. J., Dang, C., Elias, A. D., Giordano, S. H., Goetz, M. P., Goldstein, L. J., Isakoff, S. J., Krishnamurthy, J., Lyons, J., Marcom, P. K., Matro, J., Mayer, I. A., Moran, M. S., Mortimer, J., O'Regan, R. M., Patel, S. A., Pierce, L. J., Rugo, H. S., Sitapati, A., Smith, K. L., Smith, M. L., Soliman, H., Stringer-Reasor, E. M., Telli, M. L., Ward, J. H., Young, J. S., Burns, J. L., and Kumar, R. (2020). Breast cancer, version 3.2020, NCCN clinical practice guidelines in oncology. *Journal of the National Comprehensive Cancer Network*, 18(4), 452-478.

Jamal, A. K., Yaacob, W. A., and Din, L. B. (2009). Triterpenes from the root bark of *Phyllanthus columnaris*. *Australian Journal of Basic and Applied Sciences*, 3(2), 1428-1431.

Jeibouei, S., Akbari, M. E., Kalbasi, A., Aref, A. R., Ajoudanian, M., Rezvani, A., and Zali, H. (2019). Personalized medicine in breast cancer: pharmacogenomics approaches. *Pharmacogenomics and Personalized Medicine*, 12, 59-73.

Koay, Y. C., Wong, K. C., Osman, H., Eldeen, I., and Asmawi, M. Z. (2013). Chemical constituents and biological activities of *Strobilanthes crispus* L. *Records of Natural Products*, 7(1), 59-64.

Loibl, S., Poortmans, P., Morrow, M., Denkert, C., and Curigliano, G. (2021). Breast cancer. *The Lancet*, 397(10286), 1750-1769.

Martucciello, S., Balestrieri, M. L., Felice, F., dos Santos Estevam, C., Sant'Ana, A. E. G., Pizza, C., and Piacente, S. (2010). Effects of triterpene derivatives from *Maytenus rigida* on VEGF-induced Kaposi's sarcoma cell proliferation. *Chemico-Biological Interactions*, 183(3), 450-454.

Maughan, K. L., Lutterbie, M. A., and Ham, P. S. (2010). Treatment of breast cancer. *American Family Physician*, 81(11), 1339-1346.

Monkodkaew, S., Loetchutinat, C., Nuntasaen, N., and Pompimon, W. (2009). Identification and antiproliferative activity evaluation of a series of triterpenoids isolated from *Flueggea virosa* (Roxb. ex Willd.). *American Journal of Applied Sciences*, 6(10), 1800-1806.

Ndwigah, S. N., Thoithi, G. N., Mwangi, J. W., Amugune, B. K., Mugo, H. N., and Kibwage, I. O. (2013). Phytosterols from *Dombeya torrida* (J. F. Gmel.). *East and Central African Journal of Pharmaceutical Sciences*, 16(2), 44-48.

Oliveira, J. P. C., Ferreira, E. L. F., Chaves, M. H., Militão, G. C. G., Gerardo, M. V., Costa, A. M., Pessoa, C. O., de Moraes, M. O., and Costa-Lotufo, L. V. (2012). Chemical constituents of *Lecythis pisonis* and cytotoxic activity. *Brazilian Journal of Pharmacognosy*, 22(5), 1140-1144.

Shi, Q. W., Su, X. H., and Kiyota, H. (2008). Chemical and pharmacological research of the plants in genus *Euphorbia*. *Chemical Reviews*, 108(10), 4295-4327.

Siegel, R. L., Miller, K. D., and Jemal, A. (2020). Cancer statistics, 2020. *CA: A Cancer Journal for Clinicians*, 70(1), 7-30.

Su, M., Wu, X., Chung, H. Y., Li, Y., and Ye, W. (2009). Antiproliferative activities of five Chinese medicinal herbs and active compounds in *Elephantopus scaber*. *Natural Product Communications*, 4(8), 1025-1030.

Wongprayoon, P., and Charoensuksai, P. (2018). Cytotoxic and anti-migratory activities from hydroalcoholic extract of *Euphorbia lactea* Haw. against HN22 cell

line. *Thai Bulletin of Pharmaceutical Sciences*, 13(1), 69-77.

Wongrakpanich, A., and Charoensuksai, P. (2018). Induction of apoptosis in cancer cells by plants in the genus *Euphorbia*. *Thai Bulletin of Pharmaceutical Sciences*, 13(2), 1-11.

Yessoufou, K., Elansary, H. O., Mahmoud, E. A., and Skalicka-Woźniak, K. (2015). Antifungal, antibacterial and anticancer activities of *Ficus drupacea* L. stem bark extract and biologically active isolated compounds. *Industrial Crops and Products*, 74, 752-758.

SUPPLEMENTARY MATERIALS

1. Supporting information

2. Structural identification

The chemical structures of pure compounds **[1-3]** were determined by nuclear magnetic resonance (NMR) spectroscopy and mass spectrometry. The ^{1}H and ^{13}C-NMR data were recorded at 300 MHz and 75 MHz on a Brüker AVANCE 300 NMR spectrometer using TMS as an internal reference. High-resolution electrospray ionization mass spectrometry (HRESIMS) experiments were performed on a Micro TOF Brüker Daltonic mass spectrometer. The obtained ^{1}H-NMR, ^{13}C-NMR and mass spectral data of each compound (Figure S1-S9) were compared with data reported in literature. Together these compounds were identified as friedelin **[1]**, friedelan-3β-ol **[2]** and taraxerol **[3]**. Their physical and spectroscopic data were as followed.

Friedelin **[1]**: white crystals; mp 254-258 ^{o}C; ^{1}H-NMR (Figure S1) (300 MHz, $CDCl_3$) δ ppm: 2.40 (1H, m, H-6b), 2.25 (1H, q, *J* = 6.3 Hz, H-4), 1.97 (1H, m, H-1b), 1.75 (1H, m, H-6a), 1.69 (1H, m, H-1b), 1.18 (3H, s, H-28), 1.05 (3H, s, H-27), 1.01 (3H, s, H-26), 1.00 (3H,s, H-30), 0.95 (3H, s, H-29), 0.89 (3H, d, *J* = 6.3 Hz, H-23), 0.87 (3H, s, H-25), 0.73 (3H, s, H-24); ^{13}C-NMR (Figure S2) (75 MHz, $CDCl_3$) δ ppm: 213.3 (C-3), 59.5 (C-10), 58.2 (C-4), 53.1 (C-8), 42.8 (C-18), 42.1 (C-5), 41.5, (C-2), 41.3 (C-6), 39.7 (C-13), 39.3 (C-22), 38.3 (C-14), 37.4 (C-9), 36.0 (C-16), 35.6 (C-11), 35.3 (C-19), 35.0 (C-29), 32.8 (C-21), 32.4 (C-15), 32.1 (C-28), 31.8 (C-30), 30.5 (C-12), 30.0 (C-17), 28.2 (C-20), 22.3, (C-1), 20.3 (C-26), 18.7 (C-27), 18.2 (C-7), 17.9 (C-25), 14.7 (C-24), 6.8 (C-23); HRESIMS (Figure S9) *m/z* 449.3757 $[M+Na]^+$ (calcd. for $C_{30}H_{50}ONa$, 449.3760).

Friedelan-3β-ol **[2]**: white amorphous powder; mp. 274-280^{o}C; ^{1}H-NMR (Figure S3) (300 MHz, $CDCl_3$) δ ppm: 3.73, (1H, m, H-3), 1.90 (1H, m, H-2b), 1.73 (1H, dt, J = 9.6, 3.3 Hz, H-6b), 1.22 (1H, m, H-2a), 1.17 (3H, s, H-28), 1.01 (3H, s, H-27), 1.00 (3H, s, H-30), 0.99 (3H, s, H-26), 0.98 (1H, m, H-6a) 0.96 (3H, s, H-24), 0.95 (3H, s, H-29), 0.93 (3H, d, *J* = 6.0 Hz, H-23), 0.86 (3H, s, H-25); ^{13}C-NMR (Figure S4) (75 MHz, $CDCl_3$) δ ppm: 72.8 (C-3), 61.3 (C-10), 53.2 (C-8), 49.2 (C-4), 42.8 (C-18), 41.7 (C-6), 39.7 (C-14), 39.3, (C-22), 38.4 (C-13), 37.8 (C-5), 37.1 (C-9), 36.1 (C-16), 35.6 (C-11), 35.3 (C-19), 35.2 (C-2), 35.0 (C-29), 32.8 (C-21), 32.3 (C-15), 32.1 (C-28), 31.8 (C-30), 30.6 (C-12), 30.0 (C-17), 28.2 (C-20), 20.1 (C-26), 18.7 (C-27), 18.3 (C-25), 17.6, (C-7), 16.4 (C-24), 15.8 (C-1), 11.6 (C-23); HRESIMS (Figure S10) *m/z* $[M+NH_4]^+$ 446.4342 (calcd. for $C_{30}H_{52}O+NH_4^+$, 446.4356).

Taraxerol **[3]**: white crystals; mp 269-272 ^{o}C; ^{1}H-NMR (Figure S5) (300 MHz, $CDCl_3$) δ ppm: 5.53 (1H, dd, H-15, *J* = 8.2, 3.2 Hz), 3.19 (1H, m, H-3), 2.03 (1H, dt, *J* = 12.5, 3.2 Hz, H-7b), 1.96 (1H, dd, *J* = 14.7, 3.1 Hz, H-16b), 1.63 (1H, m, H-16a), 1.34 (1H, m, H-7a), 1.09 (3H, s, H-26), 0.98, (3H, s, H-23), 0.95, (3H, s, H-29), 0.93, (3H, s, H-25), 0.90, (6H, s, H-27, H-30), 0.82, (3H, s, H-28), 0.80, (3H, s, H-24); ^{13}C-NMR (Figure S6) (75 MHz, $CDCl_3$) δ ppm: 158.1 (C-14), 116.9 (C-15), 79.1 (C-3), 55.5 (C-5), 49.3 (C-9), 48.7 (C-18), 41.3 (C-7), 39.0 (C-8), 38.8 (C-4), 38.0 (C-10), 37.7 (C-1, C-16), 37.6 (C-13), 36.7 (C-16), 35.8 (C-17), 35.1 (C-22), 33.7 (C-21), 33.4 (C-29), 33.1 (C-12), 29.9 (C-30), 29.8 (C-28), 28.8 (C-20), 28.0 (C-23), 27.1 (C-2), 25.9 (C-26), 21.3 (C-27), 18.8 (C-6), 17.5 (C-11), 15.5 (C-24), 15.4 (C-25); HRESIMS (Figure S11) *m/z* 449.3768 $[M+Na]^+$ (calcd. for $C_{30}H_{50}ONa$, 449.3760).

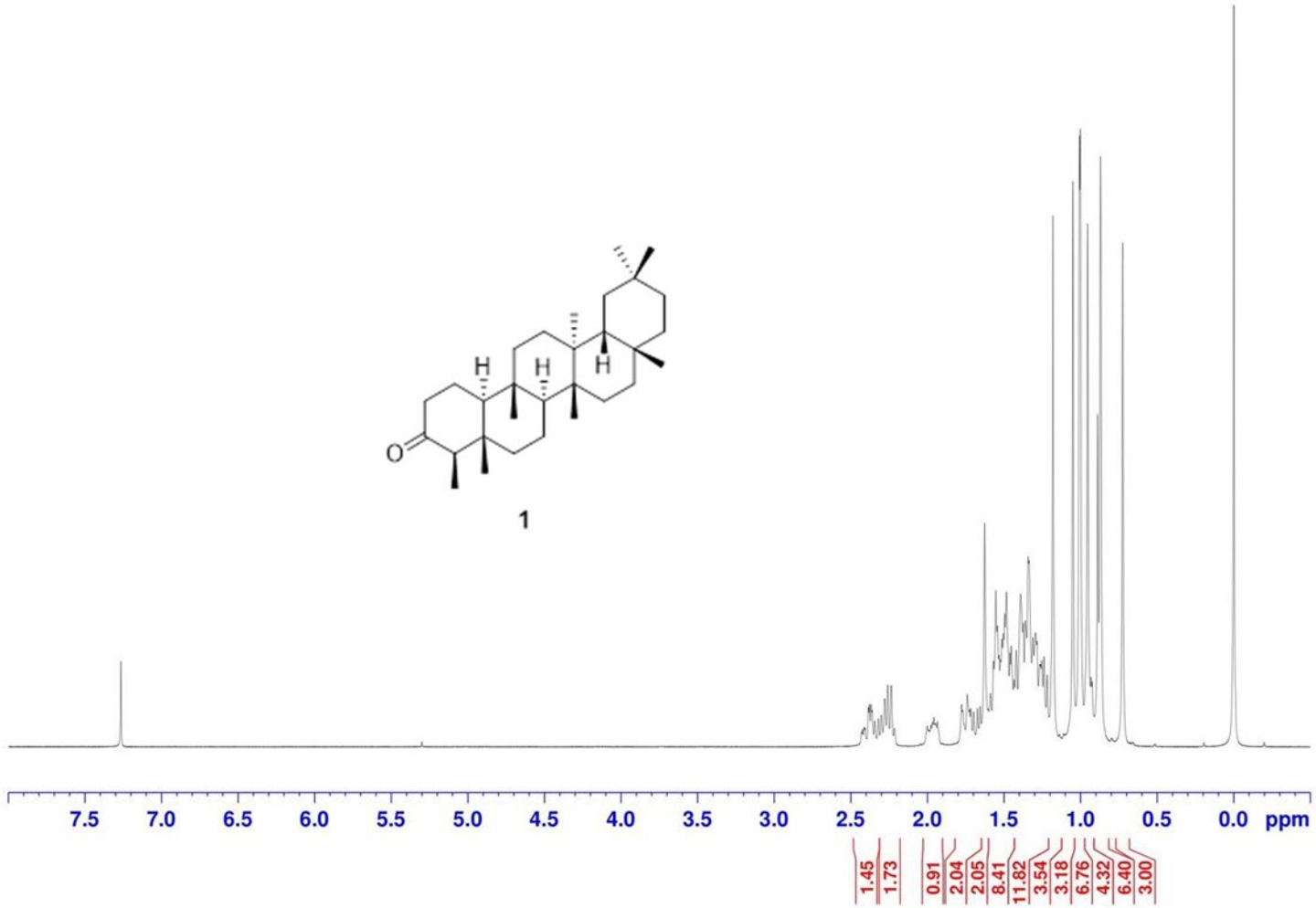

Figure S1. ^{1}H-NMR spectrum of **[1]** (300 MHz, $CDCl_3$)

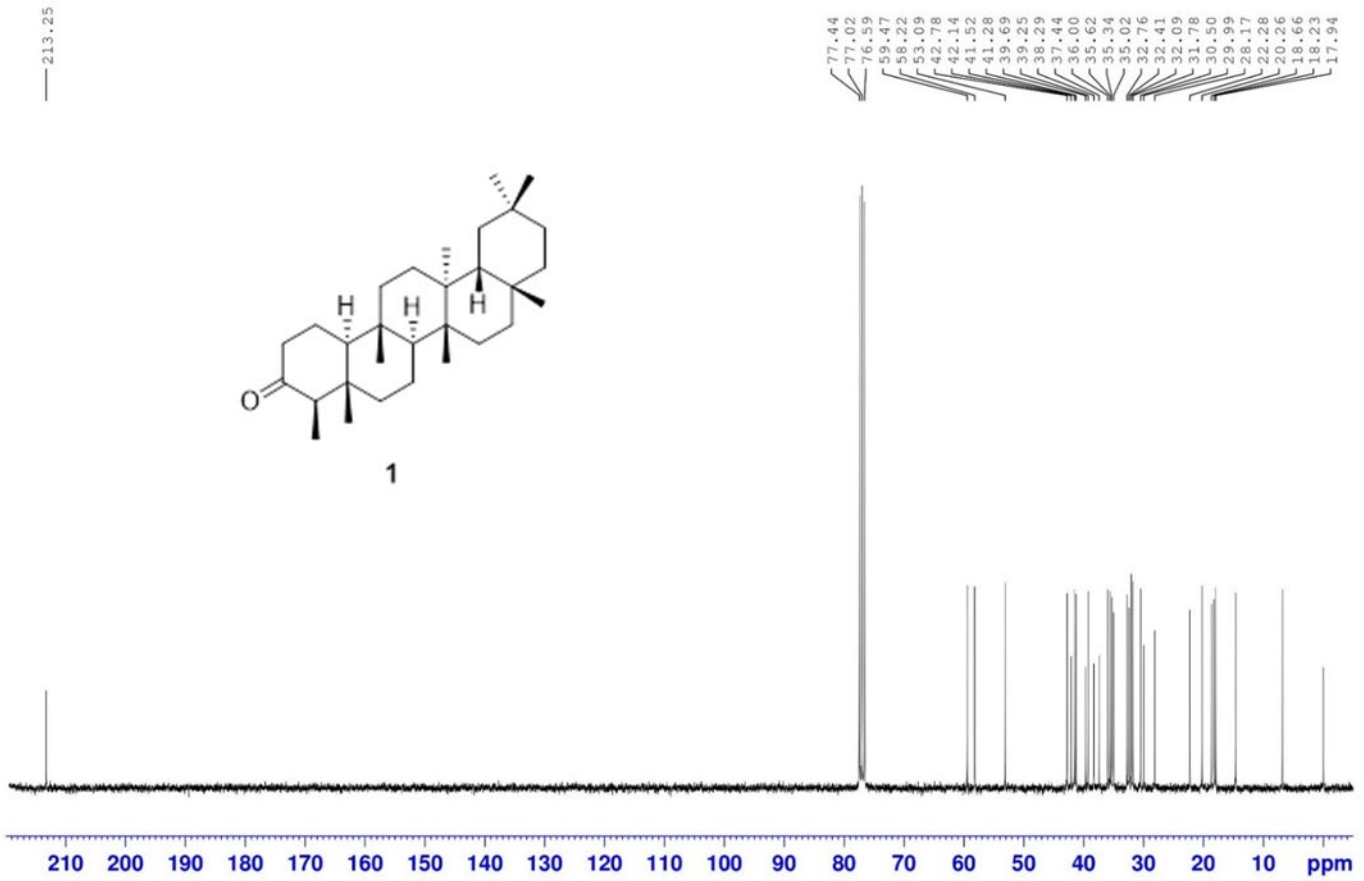

Figure S2. ^{13}C-NMR spectrum of **[1]** (75 MHz, $CDCl_3$)

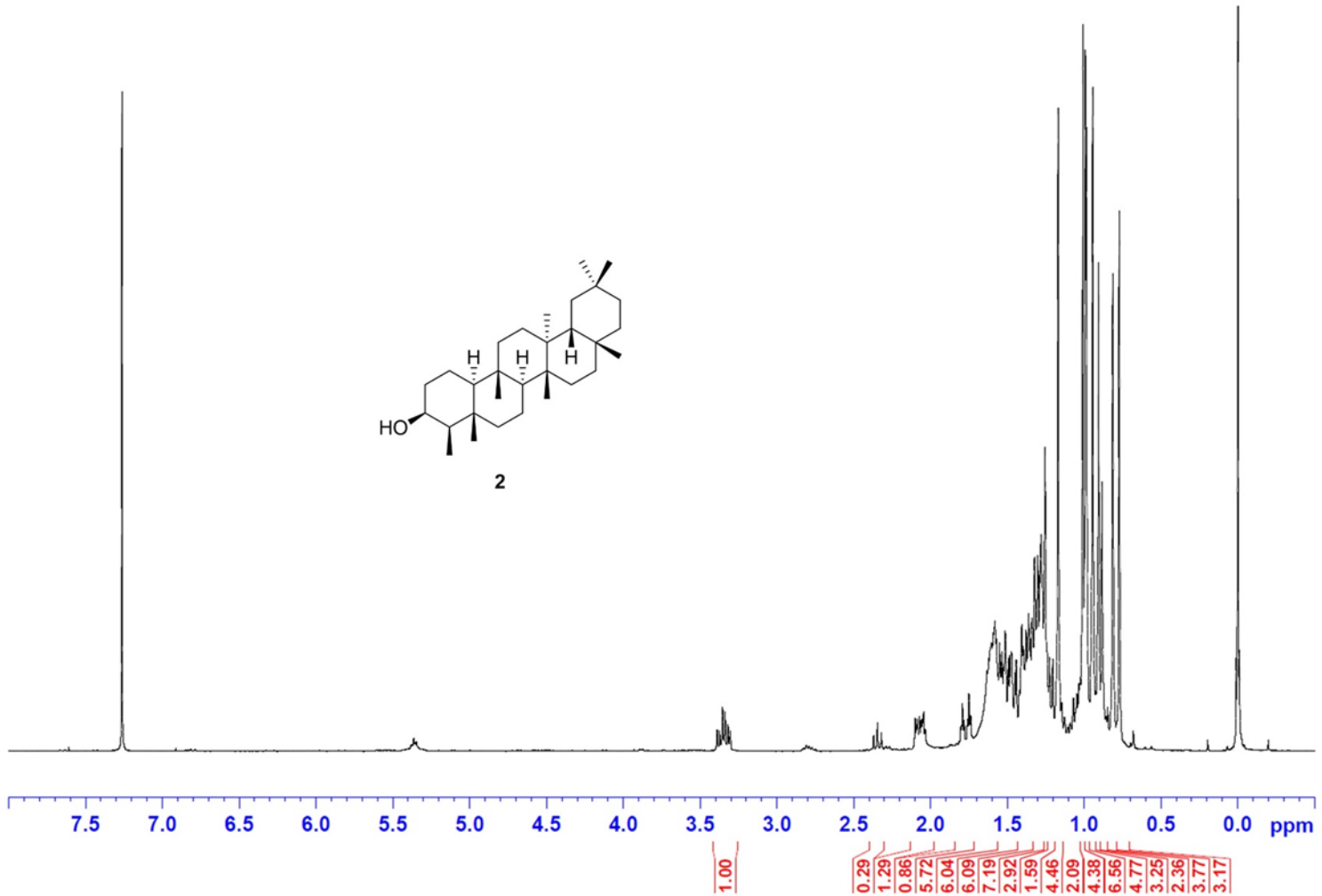

Figure S3. ^{1}H-NMR spectrum of **[2]** (300 MHz, $CDCl_3$)

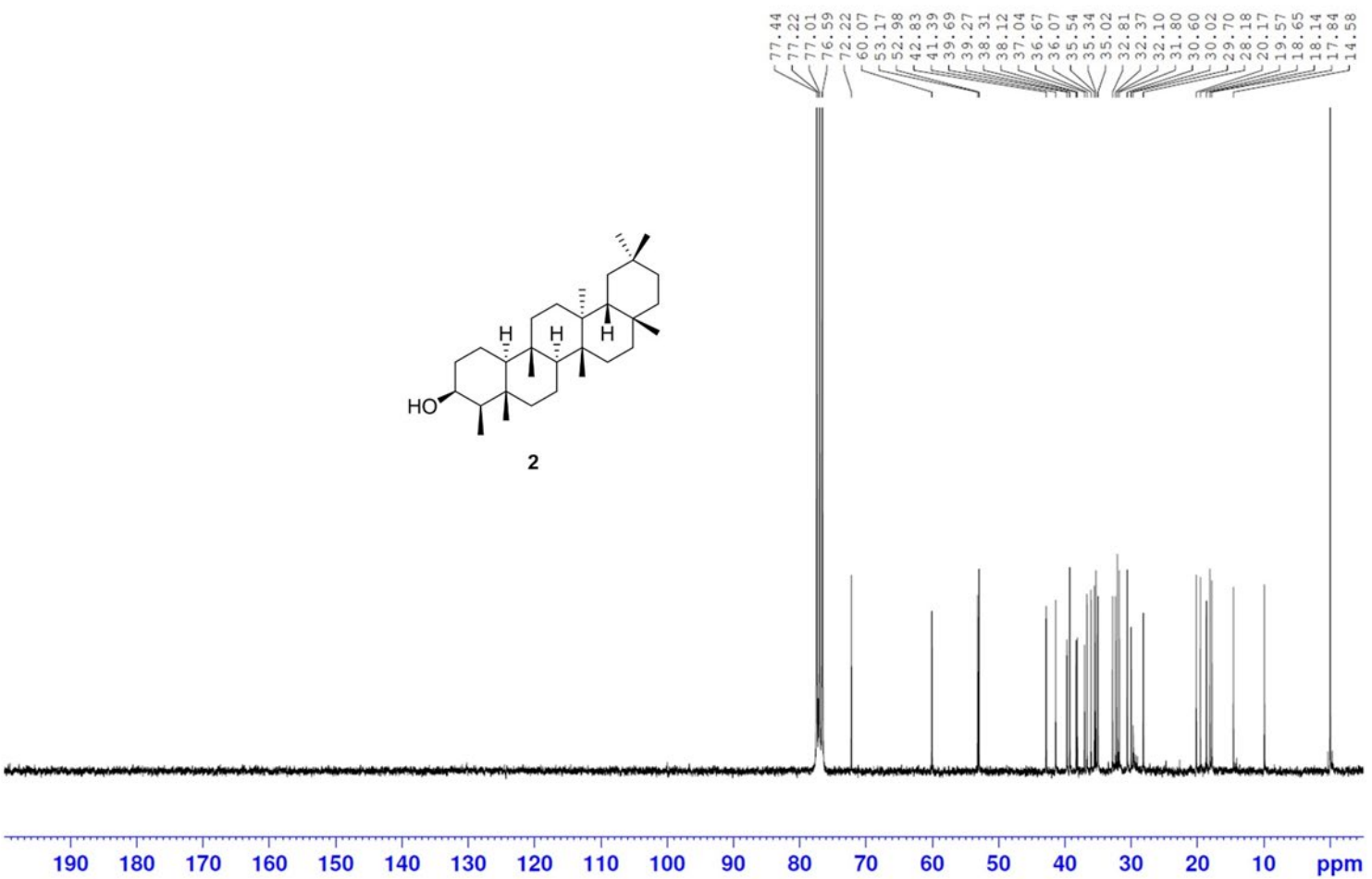

Figure S4. ^{13}C-NMR spectrum of **[2]** (75 MHz, $CDCl_3$)

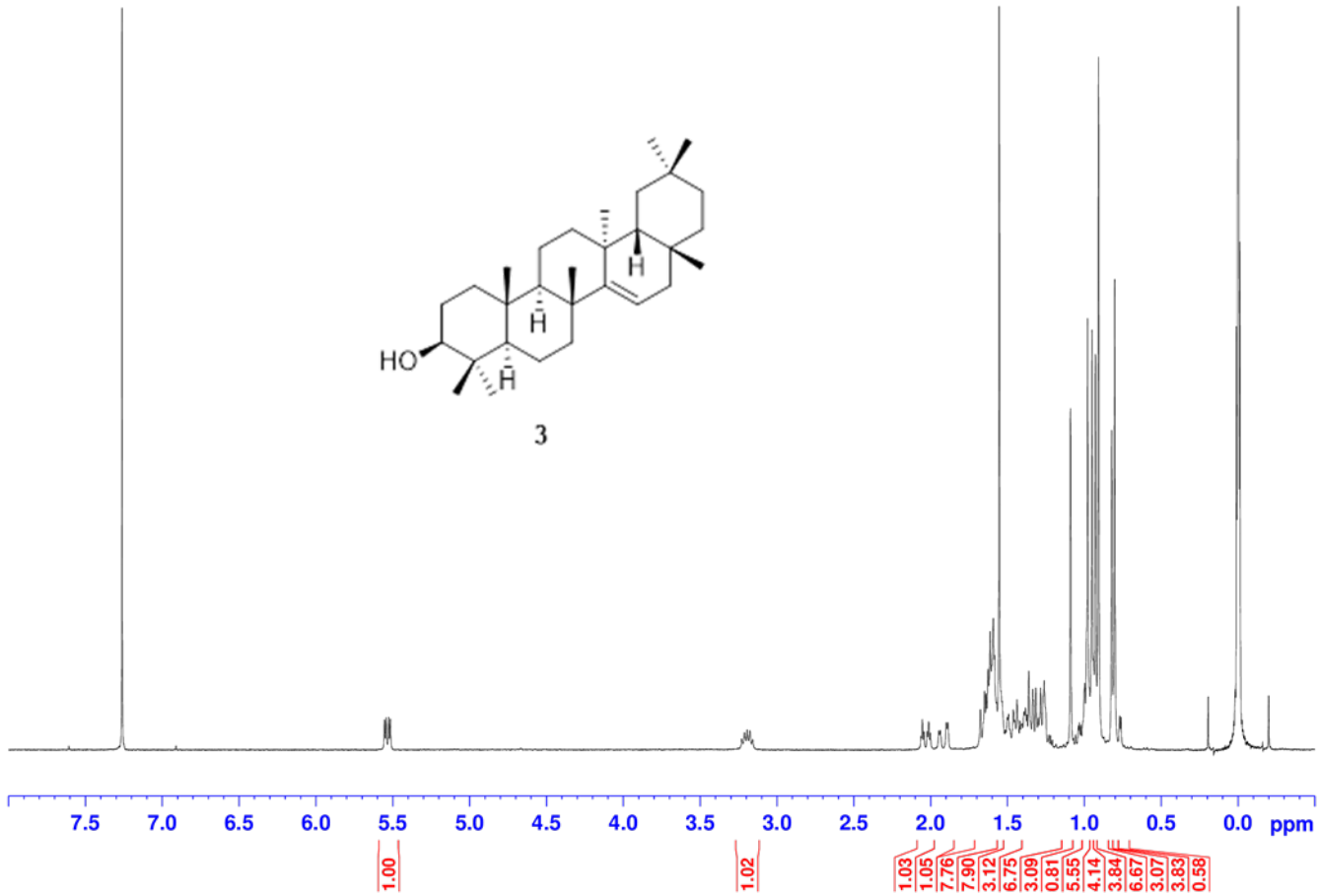

Figure S5. ^{1}H-NMR spectrum of **[3]** (300 MHz, $CDCl_3$)

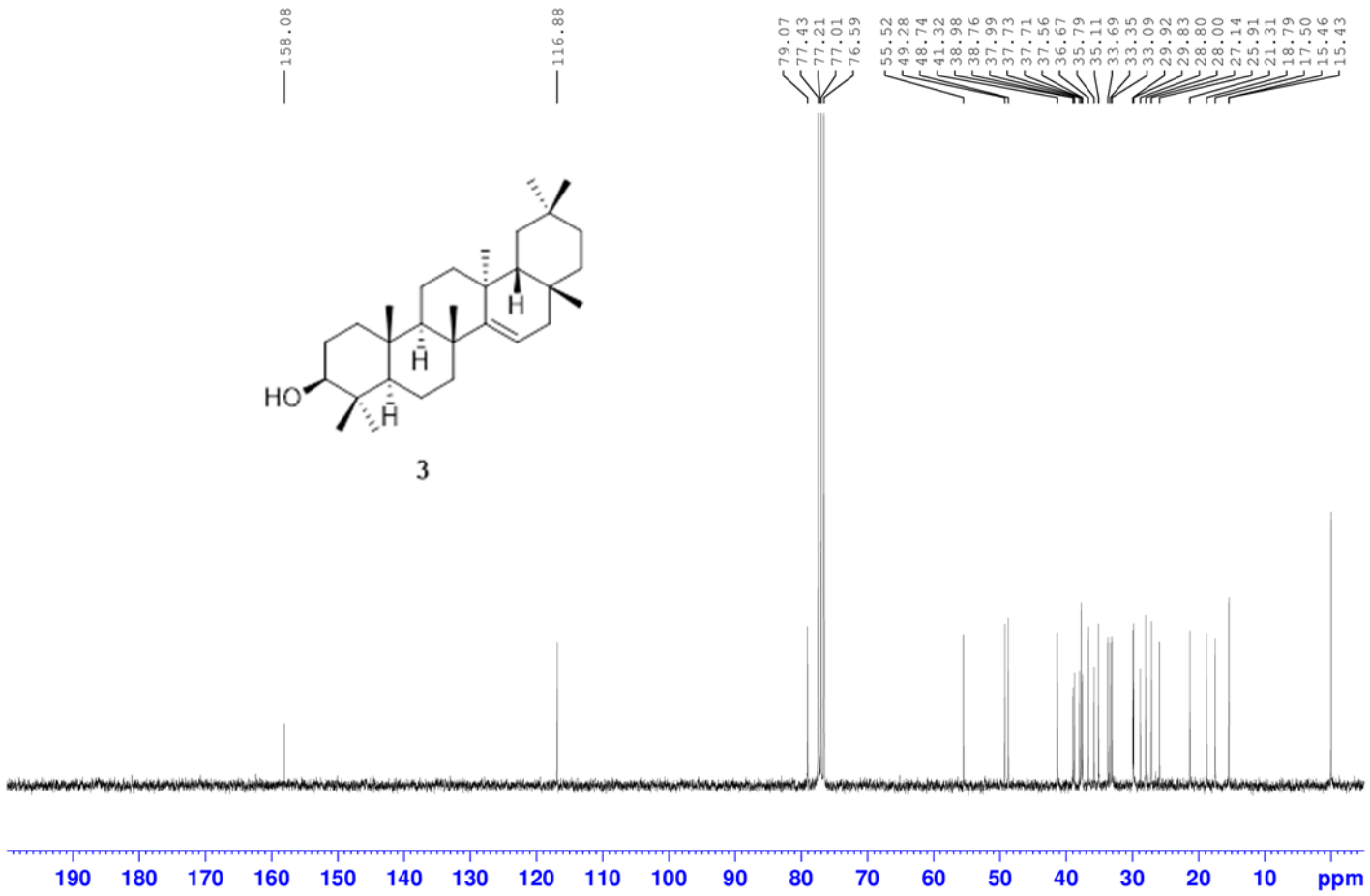

Figure S6. ^{13}C-NMR spectrum of **[3]** (75 MHz, $CDCl_3$)

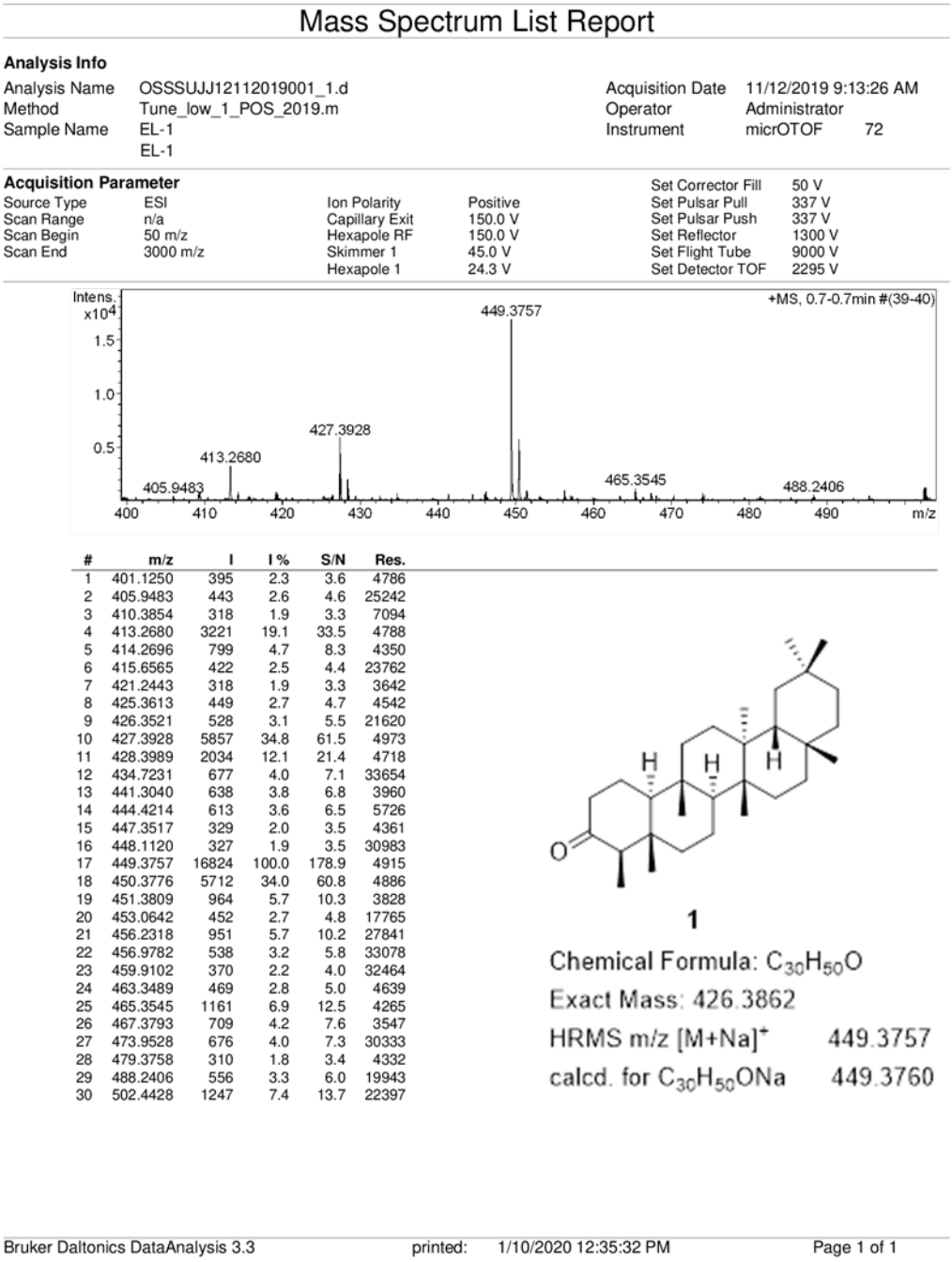

Mass Spectrum List Report

Analysis Info

Analysis Name	OSSSUJJ12112019001_1.d	Acquisition Date	11/12/2019 9:13:26 AM
Method	Tune_low_1_POS_2019.m	Operator	Administrator
Sample Name	EL-1	Instrument	micrOTOF 72
	EL-1		

Acquisition Parameter

Source Type	ESI	Ion Polarity	Positive	Set Corrector Fill	50 V
Scan Range	n/a	Capillary Exit	150.0 V	Set Pulsar Pull	337 V
Scan Begin	50 m/z	Hexapole RF	150.0 V	Set Pulsar Push	337 V
Scan End	3000 m/z	Skimmer 1	45.0 V	Set Reflector	1300 V
		Hexapole 1	24.3 V	Set Flight Tube	9000 V
				Set Detector TOF	2295 V

#	m/z	I	I %	S/N	Res.
1	401.1250	395	2.3	3.6	4786
2	405.9483	443	2.6	4.6	25242
3	410.3854	318	1.9	3.3	7094
4	413.2680	3221	19.1	33.5	4788
5	414.2696	799	4.7	8.3	4350
6	415.6565	422	2.5	4.4	23762
7	421.2443	318	1.9	3.3	3642
8	425.3613	449	2.7	4.7	4542
9	426.3521	528	3.1	5.5	21620
10	427.3928	5857	34.8	61.5	4973
11	428.3989	2034	12.1	21.4	4718
12	434.7231	677	4.0	7.1	33654
13	441.3040	638	3.8	6.8	3960
14	444.4214	613	3.6	6.5	5726
15	447.3517	329	2.0	3.5	4361
16	448.1120	327	1.9	3.5	30983
17	449.3757	16824	100.0	178.9	4915
18	450.3776	5712	34.0	60.8	4886
19	451.3809	964	5.7	10.3	3828
20	453.0642	452	2.7	4.8	17765
21	456.2318	951	5.7	10.2	27841
22	456.9782	538	3.2	5.8	33078
23	459.9102	370	2.2	4.0	32464
24	463.3489	469	2.8	5.0	4639
25	465.3545	1161	6.9	12.5	4265
26	467.3793	709	4.2	7.6	3547
27	473.9528	676	4.0	7.3	30333
28	479.3758	310	1.8	3.4	4332
29	488.2406	556	3.3	6.0	19943
30	502.4428	1247	7.4	13.7	22397

1

Chemical Formula: $C_{30}H_{50}O$

Exact Mass: 426.3862

HRMS m/z $[M+Na]^+$ 449.3757

calcd. for $C_{30}H_{50}ONa$ 449.3760

Bruker Daltonics DataAnalysis 3.3 printed: 1/10/2020 12:35:32 PM Page 1 of 1

Figure S7. HRESIMS spectrum of **[1]**

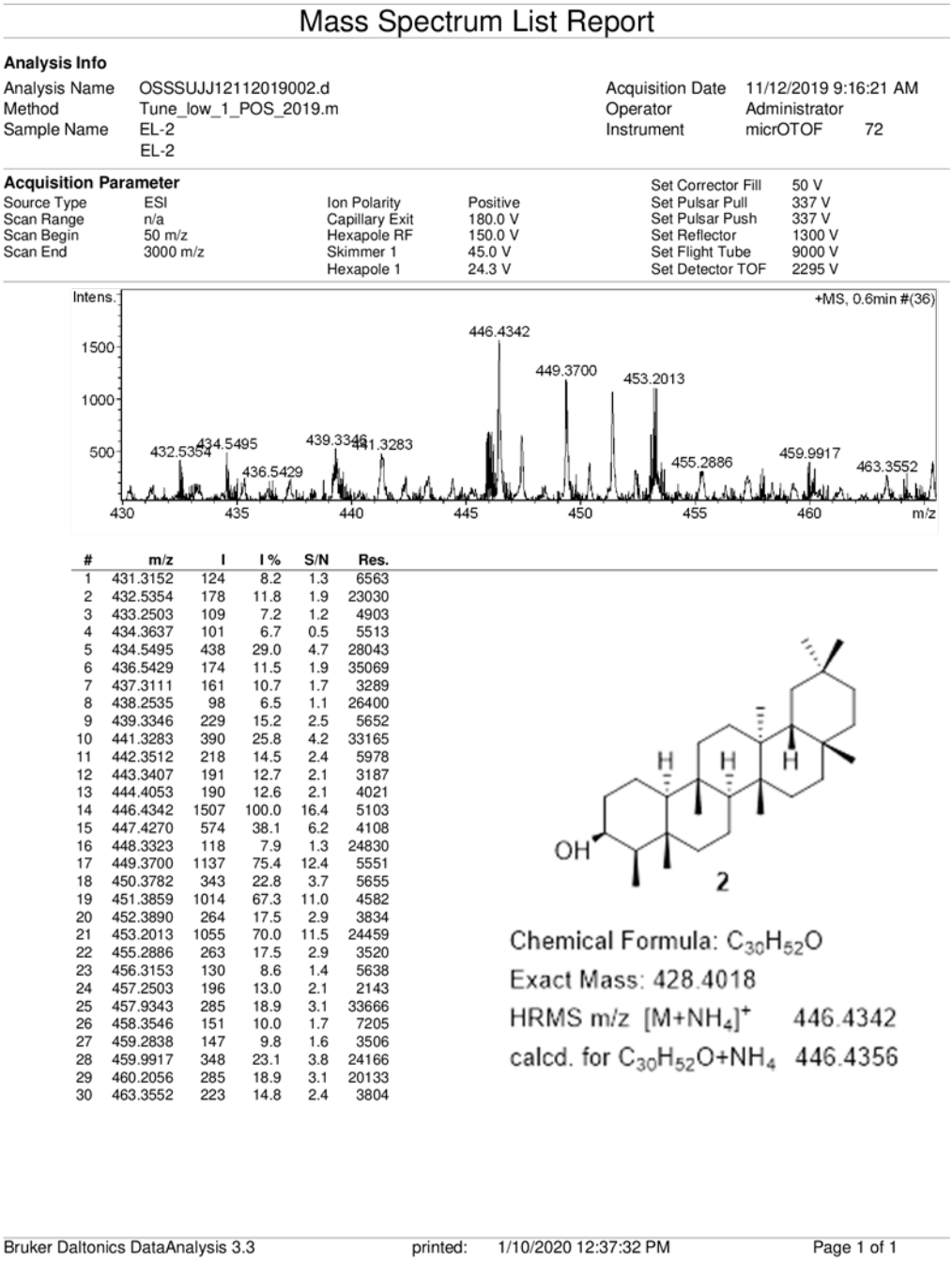

Mass Spectrum List Report

Analysis Info

Analysis Name	OSSSUJJ12112019002.d	Acquisition Date	11/12/2019 9:16:21 AM
Method	Tune_low_1_POS_2019.m	Operator	Administrator
Sample Name	EL-2	Instrument	micrOTOF 72
	EL-2		

Acquisition Parameter

Source Type	ESI	Ion Polarity	Positive	Set Corrector Fill	50 V
Scan Range	n/a	Capillary Exit	180.0 V	Set Pulsar Pull	337 V
Scan Begin	50 m/z	Hexapole RF	150.0 V	Set Pulsar Push	337 V
Scan End	3000 m/z	Skimmer 1	45.0 V	Set Reflector	1300 V
		Hexapole 1	24.3 V	Set Flight Tube	9000 V
				Set Detector TOF	2295 V

#	m/z	I	I %	S/N	Res.
1	431.3152	124	8.2	1.3	6563
2	432.5354	178	11.8	1.9	23030
3	433.2503	109	7.2	1.2	4903
4	434.3637	101	6.7	0.5	5513
5	434.5495	438	29.0	4.7	28043
6	436.5429	174	11.5	1.9	35069
7	437.3111	161	10.7	1.7	3289
8	438.2535	98	6.5	1.1	26400
9	439.3346	229	15.2	2.5	5652
10	441.3283	390	25.8	4.2	33165
11	442.3512	218	14.5	2.4	5978
12	443.3407	191	12.7	2.1	3187
13	444.4053	190	12.6	2.1	4021
14	446.4342	1507	100.0	16.4	5103
15	447.4270	574	38.1	6.2	4108
16	448.3323	118	7.9	1.3	24830
17	449.3700	1137	75.4	12.4	5551
18	450.3782	343	22.8	3.7	5655
19	451.3859	1014	67.3	11.0	4582
20	452.3890	264	17.5	2.9	3834
21	453.2013	1055	70.0	11.5	24459
22	455.2886	263	17.5	2.9	3520
23	456.3153	130	8.6	1.4	5638
24	457.2503	196	13.0	2.1	2143
25	457.9343	285	18.9	3.1	33666
26	458.3546	151	10.0	1.7	7205
27	459.2838	147	9.8	1.6	3506
28	459.9917	348	23.1	3.8	24166
29	460.2056	285	18.9	3.1	20133
30	463.3552	223	14.8	2.4	3804

Chemical Formula: $C_{30}H_{52}O$

Exact Mass: 428.4018

HRMS m/z $[M+NH_4]^+$ 446.4342

calcd. for $C_{30}H_{52}O+NH_4$ 446.4356

Bruker Daltonics DataAnalysis 3.3 printed: 1/10/2020 12:37:32 PM Page 1 of 1

Figure S8. HRESIMS spectrum of **[2]**

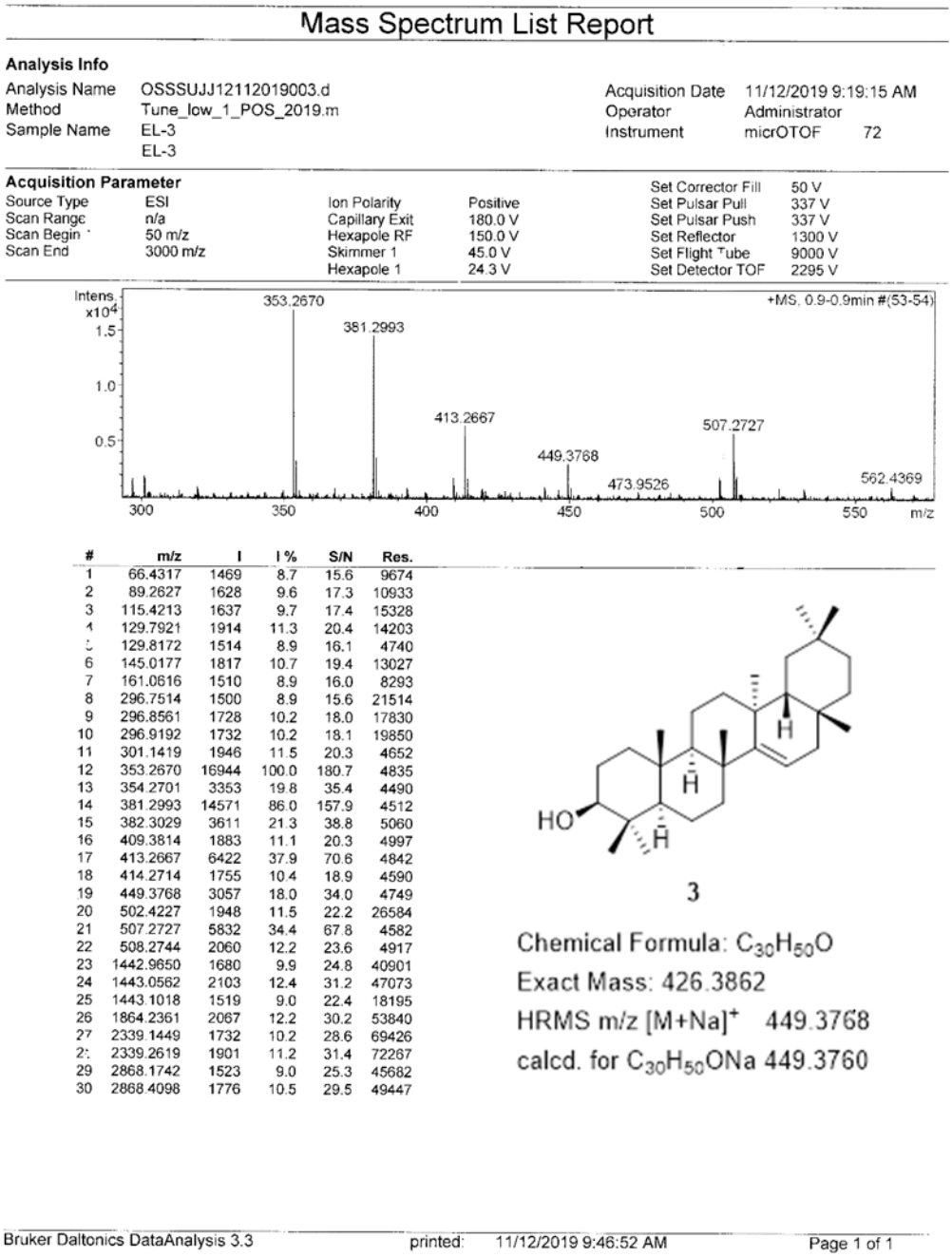

Mass Spectrum List Report

Analysis Info

Analysis Name	OSSSUJJ12112019003.d	Acquisition Date	11/12/2019 9:19:15 AM
Method	Tune_low_1_POS_2019.m	Operator	Administrator
Sample Name	EL-3	Instrument	micrOTOF 72
	EL-3		

Acquisition Parameter

Source Type	ESI	Ion Polarity	Positive	Set Corrector Fill	50 V
Scan Range	n/a	Capillary Exit	180.0 V	Set Pulsar Pull	337 V
Scan Begin	50 m/z	Hexapole RF	150.0 V	Set Pulsar Push	337 V
Scan End	3000 m/z	Skimmer 1	45.0 V	Set Reflector	1300 V
		Hexapole 1	24.3 V	Set Flight Tube	9000 V
				Set Detector TOF	2295 V

#	m/z	I	I %	S/N	Res.
1	66.4317	1469	8.7	15.6	9674
2	89.2627	1628	9.6	17.3	10933
3	115.4213	1637	9.7	17.4	15328
4	129.7921	1914	11.3	20.4	14203
5	129.8172	1514	8.9	16.1	4740
6	145.0177	1817	10.7	19.4	13027
7	161.0616	1510	8.9	16.0	8293
8	296.7514	1500	8.9	15.6	21514
9	296.8561	1728	10.2	18.0	17830
10	296.9192	1732	10.2	18.1	19850
11	301.1419	1946	11.5	20.3	4652
12	353.2670	16944	100.0	180.7	4835
13	354.2701	3353	19.8	35.4	4490
14	381.2993	14571	86.0	157.9	4512
15	382.3029	3611	21.3	38.8	5060
16	409.3814	1883	11.1	20.3	4997
17	413.2667	6422	37.9	70.6	4842
18	414.2714	1755	10.4	18.9	4590
19	449.3768	3057	18.0	34.0	4749
20	502.4227	1948	11.5	22.2	26584
21	507.2727	5832	34.4	67.8	4582
22	508.2744	2060	12.2	23.6	4917
23	1442.9650	1680	9.9	24.8	40901
24	1443.0562	2103	12.4	31.2	47073
25	1443.1018	1519	9.0	22.4	18195
26	1864.2361	2067	12.2	30.2	53840
27	2339.1449	1732	10.2	28.6	69426
28	2339.2619	1901	11.2	31.4	72267
29	2868.1742	1523	9.0	25.3	45682
30	2868.4098	1776	10.5	29.5	49447

3

Chemical Formula: $C_{30}H_{50}O$

Exact Mass: 426.3862

HRMS m/z $[M+Na]^+$ 449.3768

calcd. for $C_{30}H_{50}ONa$ 449.3760

Bruker Daltonics DataAnalysis 3.3 printed: 11/12/2019 9:46:52 AM Page 1 of 1

Figure S9. HRESIMS spectrum of **[3]**